

FAN BEAM EMISSION TOMOGRAPHY FOR LAMINAR FIRES

Yudaya Sivathanu and Jongmook Lim
En'Urga Inc., West Lafayette, IN 47906

Douglas Feikema
NASA Glenn Research Center, Cleveland, OH 44135

Introduction

Obtaining information on the instantaneous structure of turbulent and transient flames is important in a wide variety of applications such as fire safety, pollution reduction, flame spread studies, and model validation. Durao et al. (1992) has reviewed the different methods of obtaining structure information in reacting flows. These include Tunable Laser Absorption Spectroscopy (Hanson et al., 1980), Fourier Transform Infrared Spectroscopy (Best et al., 1991), and Emission Spectroscopy (Sivathanu and Gore, 1991) to mention a few.

Diagnostics with high power lasers are difficult to implement in microgravity environment. Absorption spectroscopy using either tunable laser diodes (Hanson et al., 1980) or FTIR (Best et al., 1991) can be used with deconvolution to obtain local gas species concentrations, soot volume fractions and temperatures in laminar flames. However, absorption spectroscopy requires a source, with corresponding alignment problems. The advantages of absorption spectroscopy are that it can be utilized even in low temperature flows, and is ideally suited to measure gas species concentrations (Zhang and Cheng, 1986).

Most flames emit significant radiation signatures that are used in various applications such as fire detection (Sivathanu and Tseng, 1996), light-off detection (Vaidya et al., 1982), flame diagnostics (Choi et al., 1995), etc. Radiation signatures can be utilized to maximum advantage for determining structural information in turbulent flows (Sivathanu and Faeth, 1990, Sivathanu and Gore, 1991, Sivathanu et al., 1991). Emission spectroscopy is most advantageous in the infrared regions of the spectra, principally because these emission lines arise from transitions in the fundamental bands of stable species such as CO₂ and H₂O.

Based on the above, the objective of this work was to develop a fan beam emission tomography system to obtain the local scalar properties such as temperature and mole fractions of major gas species from path integrated multi-wavelength infrared radiation measurements.

Experimental and Theoretical Method

Tomographic reconstruction of local scalar properties is based on the deconvolution of a finite number of two-dimensional path-integrated multi-wavelength radiation measurements that would be acquired by a mid-infrared spectrometer with a scanner (Spectraline Inc., Model ES100). For an axisymmetrical flame, the experimental arrangement is illustrated in Fig. 1. For each ring, unique scalars (temperature, mole fraction of CO₂ and H₂O) are defined. In the Fig.1, gas temperature, mole fraction of CO₂ and H₂O are denoted as T_i, X_{i1} and X_{i2}, respectively.

The spectral radiation intensity emitted from a homogeneous path is represented as

$$I_{\lambda} = I_{b\lambda}(1 - \tau_{\lambda}) \quad (1)$$

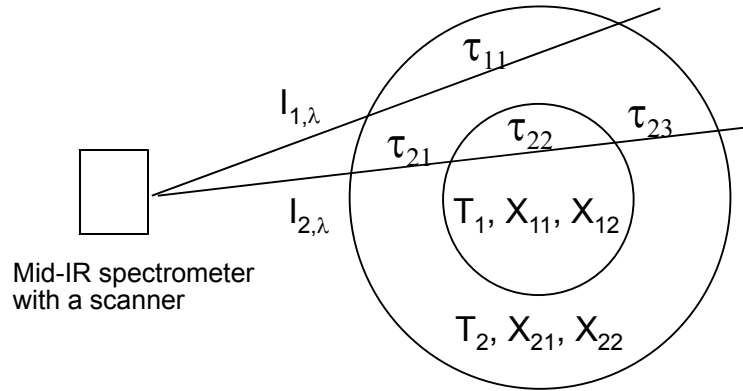


Figure 1. Schematic of Fan Beam Emission Tomography.

where $I_{b\lambda}$ is the Planck function (dependent on the gas temperature), and τ_λ is the spectral transmittance of the homogeneous path. For a given temperature and mole fractions of CO_2 and H_2O , the spectral transmittance (τ_λ) along the optical path can be calculated using a narrow band radiation model, RADCAL (Grosshandler, 1993). For the two representative homogeneous rings shown in Fig. 1, the measured path-integrated intensities are:

$$I_{1,\lambda} = I_{1,b\lambda}(1 - \tau_{11}) \quad (2)$$

$$I_{2,\lambda} = I_{1,b\lambda}[(1 - \tau_{23}) \cdot \tau_{22} \cdot \tau_{21} + (1 - \tau_{21})] + I_{2,b\lambda}(1 - \tau_{22}) \cdot \tau_{21}. \quad (3)$$

These two path-integrated intensities are calculated at several mid-infrared wavelengths. The iterative deconvolution algorithm used to obtain the local scalars from the path-integrated intensities involves two steps: (1) Calculation of the local spectral radiation intensities for all homogeneous rings, given the value of the transmittances for all segments in the optical path, and (2) Estimation of the gas temperature and mole fractions of CO_2 and H_2O from the local spectral intensities within each homogeneous ring.

A linearized MLE inversion method is used to find the three scalars in the homogeneous gas path. The estimated local temperatures and mole fractions are used to calculate the transmittances for all segments in the domain. These transmittances are then used in Step 1. This two-step process is repeated until convergence is achieved. At the first iteration, local intensities are found only considering emission and neglecting self-absorption by intervening gaseous components.

Results and Discussion

The performance of the inversion algorithm was evaluated using a synthetic dataset. The synthetic dataset consists of a 13 point radial profile of gas temperatures and mole fractions of CO_2 and H_2O . The radial profile is representative of measurements obtained in a laminar ethylene diffusion flame by Santoro et al. (1987). The major difference between the measurements (Santoro et al., 1987) and the synthetic data set is that soot is absent in synthetic data set. The path-integrated radiation intensities at 140 wavelengths (2.2-4.8 μm) are computed for 25 view angles using the RADCAL database. The diameter of the flame is 2 cm.

The synthetic and deconvoluted path-integrated intensities, at the point of convergence, for the center of the flame are shown in Fig. 2. The temperatures and gas concentrations obtained from the deconvolution algorithm and the synthetic data are shown in Fig. 3. The lines represent the synthetic data and the symbols represent the deconvoluted results.

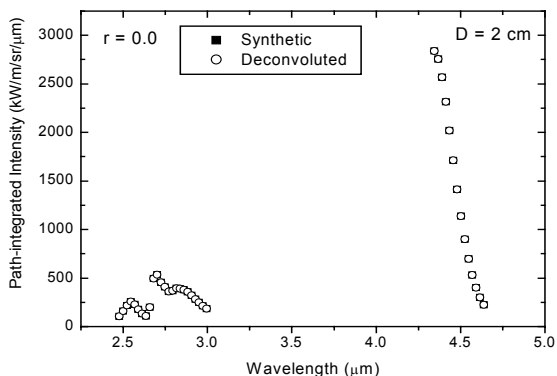


Figure 2: Synthetic and deconvoluted path integrated intensities at the center.

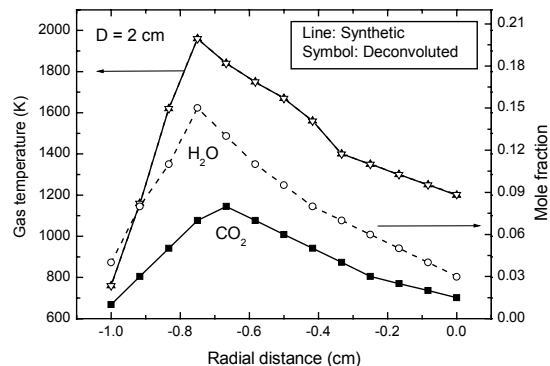


Figure 3: Synthetic and deconvoluted scalars at $x/d = 2.0$.

At the point of convergence, the spectral radiation intensities obtained from deconvolution are within 0.1% of those obtained from the synthetic data. This indicates that the deconvolution algorithm provides scalars that can match the spectral radiation intensities provided by the synthetic data set very closely. Since radiation intensities at 25 view angles were used in the deconvolution algorithm, it is possible to obtain temperatures and gas species concentrations for 13 rings. For all 13 rings, the deconvoluted scalars are within 0.1% of the synthetic data. In general, it is more difficult to obtain the scalar property at the center accurately, since the volume of gas emitting radiation is the lowest in the innermost ring. However, the results obtained are accurate to within 0.1%, even for the innermost ring.

The sensitivity of the algorithm to random noise in the intensities and wavelength was examined using the synthetic data. A random 1% noise was added to the synthetic spectral radiation intensities, and then deconvoluted using the algorithm. At the outer rings, the inversion error for the gas temperatures is less than 1%. However, the inversion error increases toward the center of the flame. At the center of the flame, the error is approximately 20%. The higher error at the center could be attributed to two reasons. The area of the center ring is approximately one tenth of the outermost ring, so the contribution of the center ring to the overall path-integrated intensities is much lower than those of outer rings. Therefore, any error in the path-integrated spectral radiation intensities could lead to high deconvolution errors at the center of the flame. The second reason for the higher deviation is that the temperature of the center ring is lower than the peak temperature. Therefore, noise contribution to the local intensity of center ring is higher since the random noise 1% is defined for peak intensities. The error in deconvoluted temperatures due to a 10 nm noise in the specified wavelength is less than 2%.

The deconvolution algorithm was then applied to spectral radiation intensity data measured from a methane/air diffusion flame. The flame was stabilized on a Santoro burner, with a methane flow rate at 7.4 cc/s and a air flow rate at 1100 cc/s. The temperatures and gas concentrations obtained from the deconvolution are shown in Figs. 4 and 5 respectively.

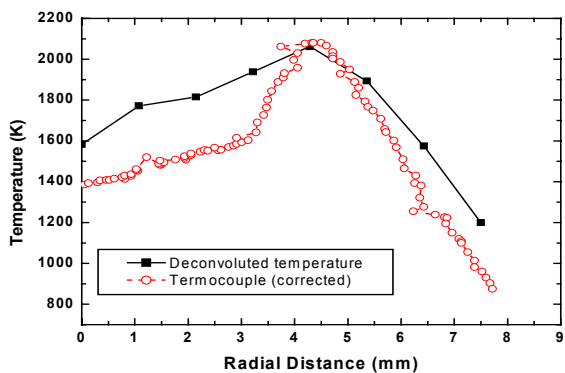


Figure 4. Temperatures obtained using fan beam emission tomography

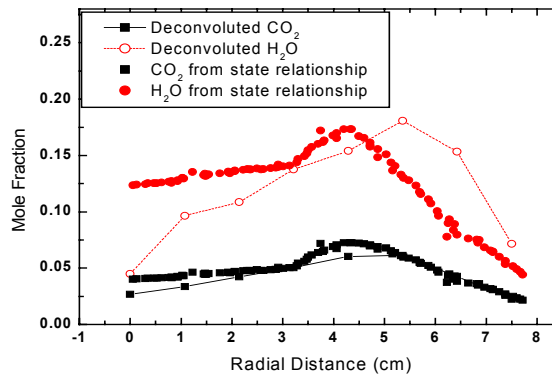


Figure 5. Gas concentrations obtained using fan beam emission tomography

The results obtained from fan beam emission tomography are in reasonable agreement with temperatures obtained from thermocouple data and gas concentrations inferred from state relationships. However, the lack of spatial resolution results in higher estimated temperatures, and consequently lower gas concentrations at the center of the flame.

Conclusions

A tomographic algorithm was developed to estimate local scalars from the multi-wavelength path-integrated spectral radiation intensities. The algorithm was evaluated using a synthetic data set. The deconvolution algorithm successfully recovers the temperature and gas concentrations within 0.1 % for a laboratory flame. The deconvolution algorithm was less successful with experimental data due to the lack of spatial resolution for the measurements.

Acknowledgement:

This research was sponsored by the NASA grant No: NAS3-01085 from NASA's Microgravity Combustion Program with Dr. Douglas Feikema as Technical Monitor.

References

- Best, P. E., Chien, P. L., Carangelo, R. M., Solomon, P. R., Danchak, M. and Ilovici, I 1991, *Combust. Flame*, vol. 85, pp. 309-318.
- Choi, M. Y., Hamins, A., Mullholland, G. W., and Kashiwagi, T., 1995, *Combust. Flame*, vol. 99, pp. 174-186
- Durao, D. F. G., Heitor, M. V., Whitelaw, J. H., and Witze, P. O., 1992, *Combustion Flow Diagnostics*, Kluwer Academic Publishers, Netherlands.
- Grosshandler, W. L., 1993, <http://fire.nist.gov/bfrlpubs/fire93/art096.html>.
- Hanson, R. K., Varghese, P. L., Schoenung, S. N., and Falcone, F. K., 1980, *Laser Probes for Combustion Chemistry*, ACS-Symposium Series, vol. 134, pp. 413-426.
- Santoro, R. J., Semerjian, Yeh, T. T., Horvath, J. J., and Semerjian, H.G., 1987, *Combust. Sci. Tech.* **53**, 89.
- Sivathanu, Y. R., and Gore, J. P., 1991, *Combust. Sci. & Tech.*, vol. 80, pp. 1-21
- Sivathanu, Y. R., and Tseng, L. K., 1998, *Fire Safety Journal*, vol. 29, pp. 301-315.
- Sivathanu, Y. R., and Faeth, G. M., 1990, *Combust. Flame*, vol. 81, pp. 150-165.
- Sivathanu, Y. R., Gore, J. P., and Dollinar, J., 1991, *Combust. Sci. Tech.*, vol. 76, pp. 45-66.
- Vardi, Y., and Lee, D., 1993, *J. R. Statist. Soc. B*, vol. 55, pp. 569-612.
- Vaidya, D. B., Horvath, J. J., and Green, A. E. S., 1982, *Applied Optics*, vol. 21, p. 3357.
- Zhang, J. Q., and Cheng, J. S., 1986, *Combust. Flame*, vol. 65, pp. 163-176.